

# Supporting Information

Rivera et al. 10.1073/pnas.1713538114

## SI Introduction

In this appendix, we derive some results regarding the coupling of atomic emitters to the phonon polaritons characteristic of polar crystals such as hBN and SiC. In particular, we consider atom-field interactions governed by the nonrelativistic Pauli–Schrodinger Hamiltonian  $H$ :

$$\begin{aligned}
 H &= H_a + H_{em} + H_{int} \\
 H_a &= \left( \sum_i \frac{\mathbf{p}_i^2}{2m_e} - \frac{e^2}{4\pi\epsilon_0 r_i} \right) \\
 H_{em} &= \sum_k \int d\mathbf{r} \int d\omega \hbar\omega \left( f_k^\dagger(\mathbf{r}, \omega) f_k(\mathbf{r}, \omega) + \frac{1}{2} \right) \\
 H_{int} &= \sum_i \frac{e}{2m} (\mathbf{p}_i \cdot \mathbf{A}(\mathbf{r}_i) + \mathbf{A}(\mathbf{r}_i) \cdot \mathbf{p}_i) + \frac{e^2}{2m} \mathbf{A}^2(\mathbf{r}_i),
 \end{aligned} \tag{S1}$$

where  $H_a$  is the atomic Hamiltonian,  $H_{int}$  is the atom-field interaction, and  $\mathbf{A}$  is the vector potential operator. The minimal-coupling interaction Hamiltonian presented above is related to the more well-known dipole interaction Hamiltonian:  $-\mathbf{d} \cdot \mathbf{E}$  + self-energy, by a unitary transformation in the long-wavelength (dipole) approximation (1). In this work, we take the dipole approximation. Thus, we take as our interaction Hamiltonian  $H_{int} = -\mathbf{d} \cdot \mathbf{E}$ . For very small wavevector PhPs, this may not be justified, but in this work, we work with parameters where the dipole approximation provides a very good approximation to the dynamics of the emitter.

The approach that we take accounts for losses via the formalism of macroscopic quantum electrodynamics (QED). The primary physical difference between QED without losses and QED with losses lies in the elementary excitations. In the lossless formalism, the excitations can be seen as quanta of electromagnetic modes. In the lossy formalism, the excitations cannot be seen as quanta of electromagnetic modes because the modes are no longer complete. Rather, the elementary excitations are point dipoles which are induced in the material. These excitations are characterized by position, frequency, and orientation. Nevertheless, as we show later, the results we obtain from this formalism in the limit of vanishing losses completely agree with the results obtained from a quantization scheme in which we take the elementary excitations to be surface PhP modes.

The electric field operator in the framework of macroscopic QED is given by (2, 3):

$$E_i(\mathbf{r}) = i \sqrt{\frac{\hbar}{\pi\epsilon_0}} \int d\mathbf{r}' \int d\omega' \frac{\omega'^2}{c^2} \sum_{k'} \sqrt{\text{Im} \epsilon(\mathbf{r}', \omega')} \left( G_{ik'}(\mathbf{r}, \mathbf{r}', \omega') \hat{f}_{k'}(\mathbf{r}', \omega') - \text{H.c.} \right), \tag{S2}$$

where  $G_{ij}$  is the dyadic Green function of the Maxwell equations, satisfying  $\nabla \times \nabla \times \mathbf{G}_i - \epsilon(\mathbf{r}, \omega) \frac{\omega^2}{c^2} \mathbf{G}_i = \delta(\mathbf{r} - \mathbf{r}') \hat{e}_i$ . The operator  $\hat{f}_j^{(\dagger)}(\mathbf{r}, \omega)$  annihilates (creates) a lossy excitation of frequency  $\omega$ , at position  $\mathbf{r}$ , and in direction  $j$ . It satisfies bosonic commutation relations, namely:  $[\hat{f}_i(\mathbf{r}, \omega), \hat{f}_j^\dagger(\mathbf{r}', \omega')] = \delta_{ij} \delta(\omega - \omega') \delta(\mathbf{r} - \mathbf{r}')$ . When applying the Fermi Golden Rule, the initial state is  $|e, 0\rangle$ , while the final states are of the form  $|g, \mathbf{x}_1 \omega_1 k_1, \dots, \mathbf{x}_N \omega_N k_N\rangle$  [S2], where  $g$  represents a ground atomic state,  $e$  represents an excited atomic state, and  $|\mathbf{x}\omega k\rangle \equiv \hat{f}_k^\dagger(\mathbf{x}, \omega)|0\rangle$  represents an excitation of the electromagnetic field.

## SI Optical Response of PhP Materials

As prescribed by Eq. S2, we must compute the Green function of a PhP supporting system. The simplest computation involves invoking the excellent approximation that the wavevector of the emitted PhPs is much larger than the photon wavelength  $\frac{\omega}{c}$ . This is the electrostatic limit.

We can compute the Green function for both an anisotropic and an isotropic polar crystal with the same methods. As is well known for a 2D-translationally invariant system, the Green function is most easily determined by writing it in Fourier space (decomposed into parallel wavevectors) and solving the Maxwell equations for each Fourier component. This Fourier integral is computed for the p-polarized polaritons; the s-polarized modes give a very weak contribution in the electrostatic limit. In the region above the dielectric slab, the Green function is known once one finds the p-polarized reflectivity of the system,  $r_p$ . In particular, the p-polarized green function takes the form (3):

$$G_{ij}^p(\mathbf{r}, \mathbf{r}', \omega) = \frac{i}{2} \frac{1}{(2\pi)^2} \int d\mathbf{q} C_{ij}^p e^{i\mathbf{q} \cdot \boldsymbol{\rho} + ik_\perp z} e^{-i\mathbf{q} \cdot \boldsymbol{\rho}' + ik_\perp z'}. \tag{S3}$$

In the electrostatic limit relevant to our calculations, the p-polarized reflectivity takes the form (4):

$$C_{ij}^p = -2i c^2 \frac{r_p q}{\omega^2} \hat{e}_i(\mathbf{q}) \hat{e}_j(\mathbf{q})^*,$$

where the polarization vectors are defined by:  $\hat{e}(\mathbf{q}) \equiv \frac{\mathbf{q} + iz}{\sqrt{2}}$ . One finds that for an isotropic slab of polar dielectric of thickness  $d$  and permittivity  $\epsilon$  with a superstrate of air and a nondispersive substrate of dielectric constant  $\epsilon_s$  that:

$$r_p = \frac{e^{2qd}(\epsilon - 1)(\epsilon_s + \epsilon) + (\epsilon + 1)(\epsilon_s - \epsilon)}{e^{2qd}(\epsilon + 1)(\epsilon_s + \epsilon) + (\epsilon - 1)(\epsilon_s - \epsilon)}. \quad [S4]$$

Similarly, one finds that for an anisotropic slab of polar dielectric (like hBN) of thickness  $d$  and permittivity  $\text{diag}(\epsilon_{\perp}, \epsilon_{\perp}, \epsilon_{\parallel})$  with a superstrate of air and a nondispersive substrate of dielectric constant  $\epsilon_s$  that:

$$r_p = \frac{(\sqrt{r}\epsilon_{\parallel} + i)(\epsilon_s + i\sqrt{r}\epsilon_{\parallel})e^{2iq\sqrt{r}d} + (\sqrt{r}\epsilon_{\parallel} - i)(\epsilon_s - i\sqrt{r}\epsilon_{\parallel})}{(\sqrt{r}\epsilon_{\parallel} - i)(\epsilon_s + i\sqrt{r}\epsilon_{\parallel})e^{2iq\sqrt{r}d} + (\sqrt{r}\epsilon_{\parallel} + i)(\epsilon_s - i\sqrt{r}\epsilon_{\parallel})} \quad [S5]$$

where  $r$  is the absolute value of the anisotropy ratio, defined by  $r = \left| \frac{\epsilon_{\perp}}{\epsilon_{\parallel}} \right|$ . The location of the poles of the imaginary part of the reflectivity in  $(\omega, q)$  space gives the dispersion relation  $\omega(q)$ . When losses are present,  $\text{Im } r_p$  is centered around the dispersion relation.

### SI Macroscopic QED at Higher Order in Perturbation Theory: Emission of Two Polaritons

In this section, we derive the frequency spectra of spontaneous emission of two excitations of the lossy electromagnetic field. These results incorporate losses and thus elucidate the contribution of quenching and polariton launching to the decay of an excited emitter. The derivation proceeds by application of the Fermi Golden Rule at second order in perturbation theory as applied to transitions between an initial state  $|e, 0\rangle$  and a continuum of final states with two excitations of the lossy electromagnetic field, i.e.,  $|g, \mathbf{x}\omega k, \mathbf{x}'\omega' k'\rangle$ . Fermi's Golden Rule for this decay reads:

$$\Gamma = \frac{2\pi^2}{\hbar} \frac{1}{2} \int d\mathbf{r} d\mathbf{r}' \int d\omega d\omega' \sum_{k, k'} \left| \sum_{i_1} \frac{\langle g, \mathbf{r}\omega k, \mathbf{r}'\omega' k' | V | i_1 \rangle \langle i_1 | V | e, 0 \rangle}{E_e - E_{i_1} + i0^+} \right|^2 \delta(\omega_0 - \omega - \omega'), \quad [S6]$$

where  $|i_1\rangle$  are intermediate states containing both the atom and field degrees of freedom. The sum is understood to be a sum over discrete degrees of freedom and an integral over continuous ones. The factor of  $1/2$  comes from the fact that when we sum over all  $\{\mathbf{r}\omega k, \mathbf{r}'\omega' k'\}$  pairs, each pair of excitations appears twice. To proceed, we express the field operators in terms of Green functions and use three facts:

i)

$$\begin{aligned} V_{i_j, i_{j-1}} &= \langle n_j, \mathbf{x}_j \omega_j k_j, \mathbf{x}_{j-1} \omega_{j-1} k_{j-1}, \dots, \mathbf{x}_1 \omega_1 k_1 | d_i E_i | n_{j-1}, \mathbf{x}_{j-1} \omega_{j-1} k_{j-1}, \dots, \mathbf{x}_1 \omega_1 k_1 \rangle \\ &= i \sqrt{\frac{\hbar}{\pi \epsilon_0}} d_{i_j}^{n_j, n_{j-1}} \frac{\omega_j^2}{c^2} \sqrt{\text{Im } \epsilon(\mathbf{x}_j, \omega_j)} G_{i_j, k_j}^*(\mathbf{r}_0, \mathbf{x}_j, \omega_j), \end{aligned}$$

ii)

$$\frac{\omega^2}{c^2} \int d\mathbf{r} \text{Im } \epsilon(\mathbf{r}, \omega) (GG^\dagger)(\mathbf{r}_0, \mathbf{r}, \omega) = \text{Im } G(\mathbf{r}_0, \mathbf{r}_0, \omega), \text{ and}$$

iii) For a photonic medium which is translationally invariant in-plane (as is the system we consider throughout the text):

$$\text{Im } G_{ij}(\mathbf{r}_0, \mathbf{r}_0, \omega) = \frac{\omega}{6\pi c} F_p(\mathbf{r}_0, \mathbf{r}_0, \omega) D_{ij},$$

where  $D = \text{diag}(1/2, 1/2, 1)$  and  $F_p$  is the Purcell factor for one-photon emission for the z-polarized dipole (frequency  $\omega$  and position  $\mathbf{r}_0$ ) near this material (5). As a reminder, this Purcell factor is equal to  $\frac{3c^3}{2\omega^3} \int dq q^2 e^{-2qz_0} \text{Im } r_p(q, \omega)$ .

Defining (note that this definition differs from that in the main text by a factor of the squared electron charge)

$$T_{ij}(\omega) = \sum_n \frac{x_j^{gn} x_i^{ne}}{\omega_e - \omega_n - \omega} + \frac{x_i^{gn} x_j^{ne}}{\omega_e - \omega_n - (\omega_0 - \omega)} = T_{ji}(\omega_0 - \omega),$$

we see that the second-order emission spectrum becomes:

$$\frac{d\Gamma}{d\omega} = \frac{4\alpha^2}{9\pi c^4} \omega^3 (\omega_0 - \omega)^3 F_p(\omega) F_p(\omega_0 - \omega) \sum_{i, j, r, s} D_{ri} D_{sj} T_{ij}(\omega) T_{rs}(\omega)^*, \quad [S7]$$

Because  $D$  is diagonal, this is simply:

$$\frac{d\Gamma}{d\omega} = \frac{4\alpha^2}{9\pi c^4} \omega^3 (\omega_0 - \omega)^3 F_p(\omega) F_p(\omega_0 - \omega) \sum_{ij} D_{ii} D_{jj} |T_{ij}|^2. \quad [S8]$$

We focus on the case in which the transition is between two  $s$  states. In that case, only the diagonal terms of  $T_{ij}$  are relevant, meaning that the above sum over  $i, j$  becomes  $\frac{3}{2} T_{zz}$ , making the differential emission rate for two lossy excitations:

$$\frac{d\Gamma}{d\omega} = \frac{2}{3\pi c^4} \alpha^2 \omega^3 (\omega_0 - \omega)^3 F_p(\omega) F_p(\omega_0 - \omega) |T_{zz}|^2 \quad [S9]$$

Using the fact that the free-space differential decay rate is given by (6):

$$\frac{d\Gamma_0}{d\omega} = \frac{4}{3\pi c^4} \alpha^2 \omega^3 (\omega_0 - \omega)^3 |T_{zz}|^2,$$

it follows that the spectral enhancement (defined in the main text) is:

$$\frac{\frac{d\Gamma}{d\omega}}{\frac{d\Gamma_0}{d\omega}} = \frac{1}{2} F_p(\omega) F_p(\omega_0 - \omega). \quad [\text{S10}]$$

By evaluating the  $T_{ij}$  tensors, we can easily go from the spectral enhancement factors to the two-photon Purcell factor by evaluating the sum over states, as we do to get the rates claimed in the main text. Moreover, the actual decay rate can easily be estimated in the case where the bandwidth of the polaritons is narrow (as is the case in what we consider) as:

$$\Gamma \approx \frac{\alpha^2}{96\pi c^4} \omega_0^6 \left| T_{zz} \left( \frac{\omega_0}{2} \right) \right|^2 \int d\omega F_p(\omega) F_p(\omega_0 - \omega), \quad [\text{S11}]$$

in the case where the emission spectrum is sharply centered at  $\frac{\omega_0}{2}$  as a result of the sharpness of the spectral enhancement.

### SI Lossless Limit: Effective Mode Expansion

This section develops a mode expansion formalism, comparing it to the Green function formalism used so far, and discusses their relative strengths and weaknesses. Although all of the decay rates that we compute can be computed through the Green function formalism presented in *SI Macroscopic QED at Higher Order in Perturbation Theory: Emission of Two Polaritons*, it is difficult to extract information such as the angular spectrum of emitted polaritons from this formalism (which we define as the angular spectrum in the lossless limit). The reason for this difficulty is that concepts like the angular spectrum are clearly most naturally computed when one assumes that the excitations coupled to are modes labeled by their direction of propagation. Therefore, to compute the angular spectrum of emitted radiation, we use a formalism different from the one used in the previous sections. We will write down field operators appropriate to the lossless situation and compute the spectrum of two-polariton emission by using Fermi's Golden Rule with these field operators.

It is known that in lossless and nondispersive dielectrics, the vector potential can be expressed in the form of a mode expansion:

$$\mathbf{A} = \sum_n \sqrt{\frac{\hbar}{2\epsilon_0\omega_n}} (\mathbf{F}_n a_n + hc),$$

where the  $\mathbf{F}_n$  are the orthonormal modes of the Maxwell equations, normalized suitably. In ref. 7, it was rigorously shown by taking the Green function formalism in the lossless limit that a mode expansion for the field operators in terms of eigenmodes (of the form above) can be derived for polaritons. In this effective mode expansion, the field modes are normalized such that:

$$\frac{\epsilon_0}{2\omega} \int d\mathbf{r} \mathbf{F}^*(\mathbf{r}) \cdot \frac{d(\epsilon_r \omega^2)}{d\omega} \cdot \mathbf{F}(\mathbf{r}) = \frac{\hbar\omega}{2}.$$

We take as the normalization or quantization volume one which is infinite in the z-direction and has area  $1 \text{ m}^2$  in the in-plane direction. In the electrostatic limit  $\frac{qc}{\omega} \gg 1$ , the fields in the vicinity of a well-localized emitter above a polar dielectric are of the form

$$\mathbf{F} \sim e^{i\mathbf{q} \cdot \boldsymbol{\rho} - qz} \hat{\mathbf{e}}(\hat{\mathbf{q}}), \quad [\text{S12}]$$

where  $\hat{\mathbf{e}}(\hat{\mathbf{q}}) \equiv \frac{\hat{\mathbf{q}} + i\hat{\mathbf{z}}}{\sqrt{2}}$ .  $\hat{\mathbf{q}}$  can be expressed as  $\cos \theta \hat{\mathbf{x}} + \sin \theta \hat{\mathbf{y}}$ . We use this fact to compute the angular spectrum of pairs of emitted PhPs in what follows.

We conclude this part of the discussion by noting that effective mode expansion was shown by proving that the denominator of the Fourier-transformed Green function in the lossless limit is proportional to the energy term in the previous equation. Although we derived this result on very general grounds (7), we explicitly show the equivalence here as a consistency check on our calculations. In Fig. S1, we compare predictions of the mode-expansion formalism and the Green function formalism taken in the zero loss limit. The particular prediction we address is the Purcell factor of a z-polarized dipole some distance away from hBN (Fig. S1, *Left and Center*) or cBN (Fig. S1, *Right*). As can be seen, aside from small numerical integration error, these predictions match extremely well. In Fig. S2, we consider the same Purcell factor, but now we compare the lossless value of the Purcell factor to the Purcell factor when realistic losses are incorporated into the Lorentz permittivities of hBN and cBN ( $\gamma = 5 \text{ cm}^{-1}$  is taken in all three cases). We can see that these predictions agree reasonably well.

Finally, in Fig. S3, we compare the value of the Purcell factor (in hBN's upper RS band) derived analytically to that computed numerically through finite-difference frequency domain simulations (COMSOL). In both cases, losses are taken into account; the distance between the atom and hBN surface is 10 nm, and the hBN thickness is 5 nm. The numerical calculations also include the effect of s-polarized waves and nonelectrostatic effects. As can be seen from Fig. S3, despite these differences, the two calculations agree quite well.

### SI Angular Spectrum of Emitted PhPs

Now, we focus on computing the angular spectrum of radiation of PhPs emitted by an excited atomic electron. In other words, we want the quantity

$$S(\omega, \theta, \theta') \equiv \frac{d\Gamma}{d\omega d\theta d\theta'}.$$

Because we want to focus only on excitation of propagating polaritons and not loss excitations, we extract the pole contribution from the imaginary part of the p-polarized reflectivity. This is equivalent to writing field operators in the lossless limit. Writing the second-order Fermi Golden Rule for the transition rate between an initial state  $|e, 0\rangle$  and the continuum of final states  $|g, \mathbf{q}\mathbf{q}'\rangle$ , we see that:

$$\frac{d\Gamma}{d\omega d\theta d\theta'} = \frac{1}{16\pi^3 \hbar^2} \frac{q(\omega)q(\omega_0 - \omega)}{v_g(\omega)v_g(\omega_0 - \omega)} \left| \sum_{i_1} \frac{\langle g, \mathbf{q}\mathbf{q}' | \mathbf{d} \cdot \mathbf{E} | i_1 \rangle \langle i_1 | \mathbf{d} \cdot \mathbf{E} | e, 0 \rangle}{E_e - E_{i_1} + i0^+} \right|^2,$$

where  $v_g$  is the group velocity,  $\frac{d\omega}{dq}$ . Inserting the definition of the operators, we find that the spectrum is given by:

$$S(\omega, \theta, \theta') = \frac{\alpha^2 c^2}{4\pi} \omega(\omega_0 - \omega) \frac{q(\omega)q(\omega_0 - \omega)}{v_g(\omega)v_g(\omega_0 - \omega)} \left| F_{\mathbf{q}}^{*i} F_{\mathbf{q}'}^{*j} T_{ij} \right|^2 \quad [\text{S13}]$$

where

$$T_{ij}(\omega) = \sum_n \frac{x_j^{gn} x_i^{ne}}{\omega_i - \omega_n - \omega} + \frac{x_i^{gn} x_j^{ne}}{\omega_i - \omega_n - (\omega_0 - \omega)} = T_{ji}(\omega_0 - \omega).$$

We now use this to extract the form of the angular spectrum of entangled photons as a function of the electronic orbitals participating in the transition. To give the reader a sense of how much control one may have over the angular spectrum of emitted photon pairs, we consider four cases. In all four, the final states are  $s$  states. But the initial states will be taken to be  $s$ ,  $d_{xy}$ ,  $d_{yz}$ , and  $d_{xz}$  states.

$s \rightarrow s$

In the case where the initial state is an  $s$  state, we have that  $T_{ij} = 0$  if  $i \neq j$ . This is because of the dipole approximation, which fixes the intermediate state to be a  $p$  state. Therefore, if  $i \neq j$ , then  $T_{ij}$  has a sum of terms like  $\langle s | x_i | p_k \rangle \langle p_k | x_j | s \rangle$ , where  $p_k = p_x, p_y, p_z$ . Each of these terms individually vanishes, and so the entire tensor vanishes. Moreover,  $T_{xx} = T_{yy} = T_{zz} \equiv T$  because  $\langle p_x | x | s \rangle = \langle p_y | y | s \rangle = \langle p_z | z | s \rangle$ . Therefore:

$$S(\omega, \theta, \theta') = |T|^2 (\cos \theta \cos \theta' + \sin \theta \sin \theta' - 1)^2 = 4|T|^2 \sin^4 \left( \frac{\theta - \theta'}{2} \right). \quad (s \rightarrow s) \quad [\text{S14}]$$

$d_{xy} \rightarrow s$

In the case where the initial state is  $d_{xy}$ , the only contributing terms are  $T_{xy}$  and  $T_{yx}$ . The argument for this statement makes use of the fact that the  $d_{xy}$  has an angular dependence that can be written in Cartesian coordinates as  $xy$ . We start proving this claim by examining the  $T_{zi}$  components. If one of the indices is  $z$ , then it will either be the case that the intermediate state must be a  $p_z$  state (to have overlap with the  $s$  state) or that there will be a matrix element of the form  $\langle p_i | z | d_{xy} \rangle$ . The first case gives zero because  $d_{xy}$  has no transition dipole moment with  $z$ . The second case also gives zero because  $d_{xy}$  has no  $z$ -polarized dipole moment with any  $p$  orbital. Thus, the  $T_{zi}$  components vanish. The  $T_{xx}$  and  $T_{yy}$  components also vanish because  $d_{xy}$  has no  $(x, y)$ -polarized dipole moment with  $p_{x,y}$ . Therefore:

$$S(\omega, \theta, \theta') = (T_{xy}(\omega) \cos \theta \sin \theta' + T_{yx}(\omega_0 - \omega) \sin \theta \cos \theta')^2. \quad (d_{xy} \rightarrow s) \quad [\text{S15}]$$

$d_{xz} \rightarrow s$  and  $d_{yz} \rightarrow s$

A nearly identical argument to the one above (replace all  $y$ 's with  $z$ 's or all  $x$ 's with  $z$ 's) yields:

$$S(\omega, \theta, \theta') = (T_{xz}(\omega) \cos \theta + T_{zx}(\omega_0 - \omega) \cos \theta')^2. \quad (d_{xz} \rightarrow s) \quad [\text{S16}]$$

$$S(\omega, \theta, \theta') = (T_{yz}(\omega) \sin \theta + T_{zy}(\omega_0 - \omega) \sin \theta')^2. \quad (d_{yz} \rightarrow s) \quad [\text{S17}]$$

## SI Validity of Perturbative Approach

Finally, we discuss the validity of perturbation theory, which we use to arrive at the results above. In this work, we showed that two-phonon-polariton emission beats one-photon emission. Were it also the case that third- and higher-order emission processes were more important than second-order processes, it would be the case that our calculations would not be representative of the full dynamics of the electron. We claim that this is not the case in our work. We estimate that three-phonon-polariton processes should be slower than two-phonon-polariton processes by  $\alpha(k_0 a)^2 F_p \frac{\Delta\omega}{\omega_0}$ , with  $F_p$  the Purcell factor the emission of a single-phonon-polariton. This factor also estimates how much slower two-phonon-polariton emission is than one-phonon-polariton emission. Taking that to be  $10^6$ ,  $\Delta\omega = \omega_0/10$ ,  $\lambda_0 = 8\mu\text{m}$ , and  $a = 1\text{nm}$ , we get that the second-order process beats the third-order process by about a factor of 2,000, making perturbation theory safe.

Although this estimate was subject to numerical assumptions, we believe this estimate is reasonable because as we saw in the main text via a concrete numerical example, if the emitter had a competing one-phonon-polariton emission process, that would happen on timescales of approximately 1 to 10 ps. Then, the two-phonon-polariton emission would be slower by about a factor of 1,000–10,000, leaving no question about the validity of perturbation theory. The ratio of first-order emission to second-order emission should be similar to the ratio between second- and third-order emission, provided all of those emissions are into polariton channels, thus lending credibility to the estimates of the previous paragraph. In the example we provide in *Extreme Enhancement of Polariton-Pair Emission Rates*, there is no competing first-order transition in our example, and that is the only reason why second-order emission becomes the most important process. Thus, we can safely reiterate that the only reason the second-order emission is dominant is not because we are in a nonperturbative regime, but because the first-order emission will be effectively unenhanced. This situation is analogous to a situation in atomic physics (1) where the hydrogen 2S state can decay either by a first-order magnetic dipole transition or a second-order two-photon electric dipole decay. The former is anomalously slow (practically forbidden), so the latter dominates the dynamics. Nevertheless, even higher-order dynamics are known to be negligible in the decay dynamics of the 2S state.

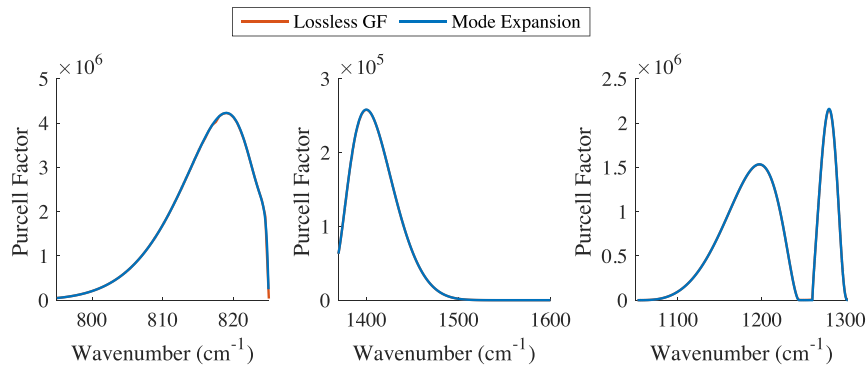


**Fig. S1.** Comparison of lossless green function formalism and mode expansion. Purcell factors calculated for the lower RS band of hBN for an hBN thickness of 2 nm and emitter-surface separation of 10 nm (*Left*), the upper RS band of hBN for an hBN thickness of 2 nm and emitter-surface separation of 10 nm (*Center*), and the RS band of cBN for a cBN thickness of 5 nm and emitter-surface separation of 10 nm (*Right*).

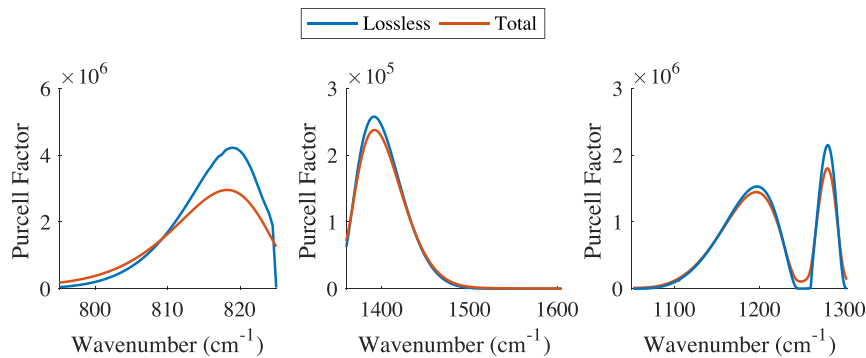


**Fig. S2.** Comparison of green function formalism with losses and mode expansion. Purcell factors calculated for the lower RS band of hBN for an hBN thickness of 2 nm and emitter-surface separation of 10 nm (*Left*), the upper RS band of hBN for an hBN thickness of 2 nm and emitter-surface separation of 10 nm (*Center*), and the RS band of cBN for a cBN thickness of 5 nm and emitter-surface separation of 10 nm (*Right*).

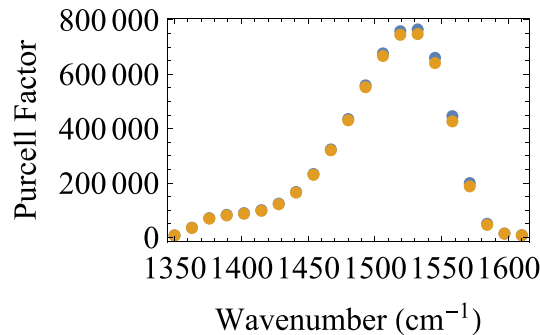


**Fig. S3.** Agreement of analytical and numerical approaches. Comparison of analytic calculation for p-polarized Purcell factor including losses in the electrostatic limit with finite-difference frequency domain (COMSOL) calculation of the Purcell factor for hBN of thickness 5 nm surrounded by air and an emitter 10 nm away from the top surface.

1. Cohen-Tannoudji C, Dupont-Roc J, Grynberg G, Thieckstun P (1992) *Atom-Photon Interactions Basic Processes and Applications* (Wiley Online Library, New York).
2. Knöll L, Scheel S, Welsch D-G (2001) QED in dispersing and absorbing media. *Coherence and Statistics of Photons and Atoms*, ed Peřina J (Wiley, New York), Sect 7.3.
3. Scheel S, Yoshi Buhmann S (2008) Macroscopic quantum electrodynamics—concepts and applications. *Acta Pys Slovaca*, 58:675–809.
4. Rivera N, Kaminer I, Zhen B, Joannopoulos JD, Soljačić M (2016) Shrinking light to allow forbidden transitions on the atomic scale. *Science* 353:263–269.
5. Koenderink AF (2010) On the use of Purcell factors for plasmon antennas. *Optic Lett* 35:4208–4210.
6. Breit G, Teller E (1940) Metastability of hydrogen and helium levels. *Astrophys J* 91:215.
7. Lin X, et al. (2016) Tailoring the energy distribution and loss of 2D plasmons. *New J Phys* 18:105007.